

## Homodimerization and Heteroassociation of 6-*O*-(2-Sulfonato-6-naphthyl)- $\gamma$ -cyclodextrin and 6-Deoxy-(pyrene-1-carboxamido)- $\beta$ -cyclodextrin

Joon Woo Park,\* Hee Eun Song, and Soo Yeon Lee

Department of Chemistry, Ewha Womans University, Seoul 120-750, Korea

jwpark@mm.ewha.ac.kr

Received May 12, 2003

6-*O*-(2-Sulfonato-6-naphthyl)- $\gamma$ -cyclodextrin (**1**) and 6-deoxy-(pyrene-1-carboxamido)- $\beta$ -cyclodextrin (**2**) were prepared. Homodimerizations of **1** and **2** and heteroassociation between **1** and **2** were investigated by  $^1\text{H}$  NMR, circular dichroism, and fluorescence spectroscopic methods. The compounds **1** and **2** form head-to-head dimers with dimerization constants of  $140 \pm 50$  and  $270 \pm 70 \text{ M}^{-1}$ , respectively. We also determined the association constants of **1** with  $\beta$ -CD as  $270 \pm 20 \text{ M}^{-1}$  and **2** with  $\gamma$ -CD as  $100 \pm 30 \text{ M}^{-1}$  from fluorescence and circular dichroism titration data, respectively. The heteroassociation between **1** and **2** was manifested in increased circular dichroism ellipticities of **2**, downfield shift of the H-2 proton of the pyrene group of **2**, and upfield shift of the H-5 proton of the naphthyl group of **1** upon mixing **1** and **2**. The analysis of circular dichroism titration data of **2** with **1** gave the association constant as  $9300 \pm 1600 \text{ M}^{-1}$ . The NMR and circular dichroism spectra suggested that the naphthyl group of **1** is deeply included into the  $\beta$ -CD cavity of **2**, while the pyrene group of **2** is partially inserted in the  $\gamma$ -CD cavity of **1** in the complex. The energy-minimized structure from molecular modeling of the complex supports this. We believe that the facile heteroassociation of two cyclodextrin derivatives having different sizes of cavity and pendant group could be utilized as a useful strategy for assembling functionalized CDs for various applications.

### Introduction

Cyclodextrins (CDs) are cyclic oligosaccharides commonly composed of 6, 7, or 8 D-glucose units, called  $\alpha$ -,  $\beta$ -, and  $\gamma$ -CD, respectively, which differ in cavity sizes. CDs form inclusion complexes with a variety of organic compounds in aqueous media and have been widely used as novel media for chemical reactions, building blocks, and functional units of supramolecules.<sup>1</sup> Photo- or electroactive groups have been attached to CDs to obtain photo- or electroresponsive host molecules. When the pendant group has the proper size, the group is self-included into the cavity of the parent CD<sup>2-5</sup> or of the counter molecules forming dimers<sup>6-12</sup> or oligomeric su-

pramolecular structures.<sup>12,13</sup> External guest molecules compete with the appended group for the CD cavity making the CD derivatives responsive to the guest. With photoisomerizable or electroactive pendant groups, it was also shown that the assemblies respond to external light<sup>5,10</sup> or electrical stimuli.<sup>7</sup>

It has been shown that dimers<sup>7-12</sup> and cyclic daisy chains<sup>12,13</sup> of CD derivatives are stabilized by mutual cooperative inclusion of pendant groups into CD cavities of counter molecules. Such cooperative inclusion would allow one to overcome intrinsic low binding affinity of

(1) For compilations of recent works on cyclodextrins and their derivatives, see: (a) Szejtli, J.; Osa, T. In *Comprehensive Supramolecular Chemistry*; Atwood, J. L., Davies, J. E. D., Vögtle, D., Eds.; Elsevier: Oxford, UK, 1996; Vol. 3. (b) D'Souza, V. T.; Lipkowitz, K. B., Eds. *Chem. Rev.* **1998**, *98*, 1741–2076.

(2) Easton, C. J.; Lincoln, S. F. *Modified Cyclodextrins: Scaffolds and Templates for Supramolecular Chemistry*; Imperial College Press: London, UK, 1999.

(3) (a) Xie, H. Z.; Wu, S. K. *Supramol. Chem.* **2001**, *13*, 545. (b) Li, D. B.; Ng, S.-C.; Novak, I. *Tetrahedron Lett.* **2002**, *43*, 1871.

(4) Park, K. K.; Kim, Y. S.; Lee, S. Y.; Song, H. E.; Park, J. W. *J. Chem. Soc., Perkin Trans. 2* **2001**, 2114 and references therein.

(5) Fukushima, M.; Osa, T.; Ueno, A. *J. Chem. Soc., Chem. Commun.* **1991**, 15.

(6) McAlphine, S. R.; Garcia-Garibay, M. A. *J. Am. Chem. Soc.* **1998**, *120*, 4269.

(7) Mirzozian, A.; Kaifer, A. E. *Chem. Commun.* **1999**, 1603.

(8) (a) Gao, X.-M.; Tong, L.-H.; Zhang, Y.-L.; Hao, A.-Y.; Inoue, Y. *Tetrahedron Lett.* **1999**, *40*, 969. (b) Gao, X.-M.; Zhang, Y.-L.; Tong, L.-H.; Zhang, Ye, Y.-H.; Ma, X.-Y.; Liu, W.-S.; Inoue, Y. *J. Inclusion Phenom. Macrocyclic Chem.* **2001**, *39*, 77.

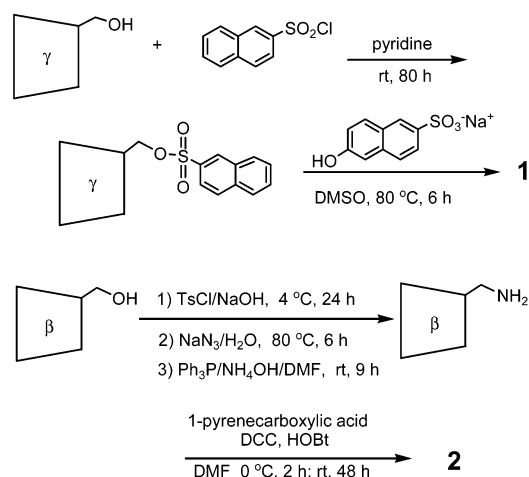
(9) (a) Park, J. W.; Choi, N. H.; Kim, J. H. *J. Phys. Chem.* **1996**, *100*, 769. (b) Fujimoto, T.; Sakata, Y.; Kaneda, T. *Chem. Commun.* **2000**, 2143. (c) de Jong, M. R.; Berthault, P.; van Hoek, A.; Visser, A. J. W. G.; Huskens, J.; Reinhoudt, D. N. *Supramol. Chem.* **2002**, *14*, 143.

(10) (a) Fujimoto, T.; Nakamura, A.; Inoue, Y.; Sakata, Y.; Kaneda, T. *Tetrahedron Lett.* **2001**, *42*, 7987. (b) Lecourt, I.; Mallet, T. M.; Sinay, P. *Tetrahedron Lett.* **2002**, *43*, 5533.

(11) Park, J. W.; Song, H. E.; Lee, S. Y. *J. Phys. Chem. B* **2002**, *106*, 5177.

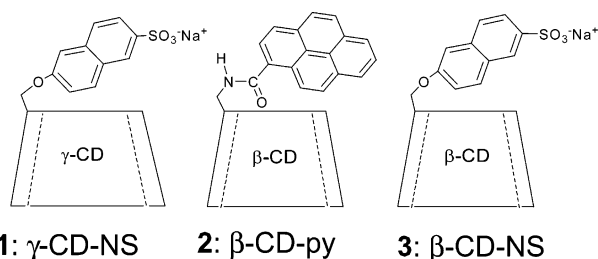
(12) Fujimoto, T.; Sakata, Y.; Kaneda, T. *Chem. Lett.* **2000**, 764.

(13) (a) Petteer, R. C.; Salek, J. S.; Sikorski, C. T.; Kumaravel, G.; Lin, F. T. *J. Am. Chem. Soc.* **1990**, *112*, 3860. (b) Hoshino, T.; Miyauchi, M.; Kawaguchi, Y.; Yamaguchi, H.; Harada, A. *J. Am. Chem. Soc.* **2000**, *122*, 9876. (c) Bügler, J.; Sommerdijk, N. A. J. M.; Visser, A. J. W. G.; van Hoek, A.; Nolte, R. J. M.; Engbersen, J. F. J.; Reinhoudt, D. N. *J. Am. Chem. Soc.* **1999**, *121*, 28. (d) Liu, Y.; Zhang, H.-Y.; Diao, C.-H. *Org. Lett.* **2003**, *5*, 251.

SCHEME 1. Synthetic Routes of **1** and **2**

pendant groups to the CD cavity for effective assembling of CD derivatives. It is expected that two dissimilar CD derivatives would form a heterocomplex if there is a complementary relationship between the pendant group of one CD derivative and the CD cavity of the other derivative. This could provide a useful strategy for obtaining novel supramolecular structures based on CDs.

In this paper, we report homodimerization and heteroassociation behaviors of 6-*O*-(2-sulfonato-6-naphthyl)- $\gamma$ -CD (**1**) and 6-deoxy-(pyrene-1-carboxamido)- $\beta$ -CD (**2**). The behaviors were compared with those of 6-*O*-(2-sulfonato-6-naphthyl)- $\beta$ -CD (**3**), which shows a strong tendency of homodimerization.<sup>11</sup> The CD derivatives were chosen since pyrene and naphthalene-tethered CDs have been widely used as fluorescent and photoactive hosts,<sup>1,2</sup> and the sizes of pyrene and naphthalene rings fit well with  $\gamma$ -CD and  $\beta$ -CD cavities, respectively,<sup>14</sup> enabling one to expect a facile heteroassociation between **1** and **2**.



## Results and Discussion

The synthetic routes for **1** and **2** are shown in Scheme 1. Compounds **1** and **2** were obtained in 24% yield from mono-6-*O*-(2-naphthalenesulfonyl)- $\gamma$ -CD (**4**) and 40% yield from  $\beta$ -CD-NH<sub>2</sub>, respectively.

We first describe the homodimerization behaviors of **1** and **2**, and then associations of **1** with  $\beta$ -CD and **2** with  $\gamma$ -CD. Finally, we present the results of heteroassociation between **1** and **2**. The equilibria and the association constants studied in this work are summarized in Scheme 2.

(14) (a) Inoue, Y.; Hakushi, T.; Liu, Y.; Tong, L.-H.; Shen, B.-J.; Jin, D.-S. *J. Am. Chem. Soc.* **1993**, *115*, 475. (b) Rekharsky, M. V.; Inoue, Y. *Chem. Rev.* **1998**, *98*, 1875.

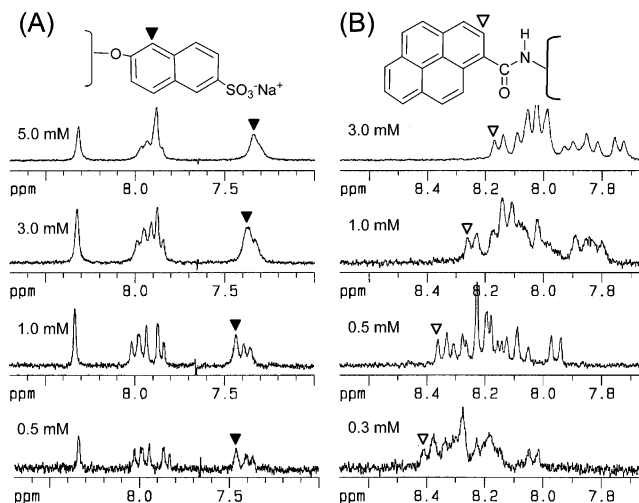
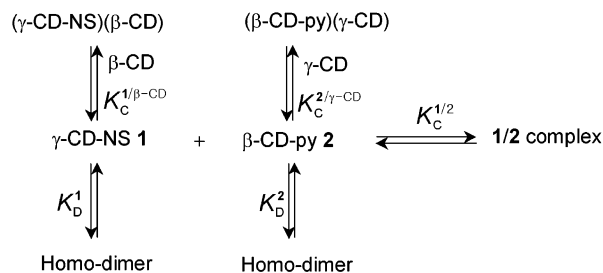


**FIGURE 1.** <sup>1</sup>H NMR spectra of the aromatic region of  $\gamma$ -CD-NS **1** (A) and  $\beta$ -CD-py **2** (B) in D<sub>2</sub>O. The concentrations of CD derivatives are shown in the figures. The symbols ▼ and ▽ indicate the signals from the H-5 proton of naphthyl and the H-2 proton of pyrenyl groups, respectively. The signal of the H-7 proton of **1** appears as a doublet near 7.4 ppm.

## SCHEME 2. The Equilibria and Association Constants Studied



**Homodimerizations of 1 and 2.** The homoassociation behaviors of **1** and **2** were investigated from the concentration dependence of their spectroscopic properties. The compound **1** exhibits strong fluorescence around 350 nm, but the fluorescence intensity ( $I_f$ ) was virtually proportional to the concentration up to 0.020 mM. The circular dichroism (c.d.) spectrum of **1** showed positive dichroic peaks around 320, 270, and 235 nm (vide intra) and resembles that of the monomeric form of **3**, in which the naphthyl group is outside of the  $\beta$ -CD cavity.<sup>11</sup> Although we observed that the molar ellipticity [ $\theta$ ] at 320 nm decreases about 20% when the concentration of **1** is varied from 0.04 to 2.0 mM, the spectral change was not sufficient enough to determine the homoassociation constant of **1** with reasonable accuracy. These results indicate that the self-association constant of **1** is too small to be measured by either fluorescence or c.d. spectroscopic method. Thus, we tried to determine the association constant of **1** by the NMR method, which makes it possible to investigate the association at a much higher concentration range.

Figure 1A shows the concentration-dependent <sup>1</sup>H NMR spectra of **1**. At low concentration, the spectrum is similar to that of the monomeric form of **3** obtained from disaggregating the dimer by the addition of *n*-octyl sulfate.<sup>11</sup> As the concentration is increased, upfield shifts of the signals from H-5 and H-7 protons of the naphthyl

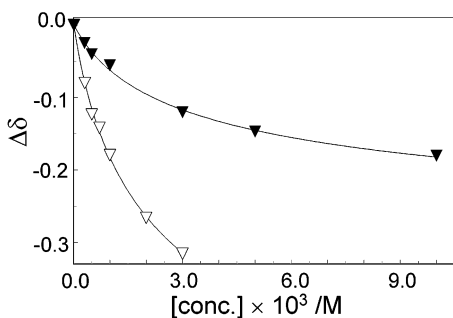


**FIGURE 2.** Concentration dependences of  $^1\text{H}$  NMR signals of H-5 proton of  $\gamma$ -CD-NS **1** ( $\blacktriangledown$ ) and H-2 protons of  $\beta$ -CD-py **2** ( $\nabla$ ). The  $\Delta\delta$  values are given with respect to the chemical shifts of the corresponding peaks of the monomeric forms obtained from the fittings, 7.490 ppm for the H-5 proton of **1** and 8.456 ppm for the H-2 proton of **2**. We were not able to take the NMR spectrum of **2** at higher concentration due to the solubility limit.

group are clearly seen. This is analogous to the observations with **3**<sup>11</sup> and 3-*O*-(2-methylnaphthyl)- $\beta$ -CD.<sup>6</sup> The concentration ( $C_{\text{tot}}$ )-dependent  $^1\text{H}$  NMR signal of the H-5 proton (Figure 2) fitted well to the dimerization scheme (eq 1) and gave the dimerization constant ( $K_{\text{D}}^1$ ) as  $140 \pm 50 \text{ M}^{-1}$  and  $\delta_{\text{mon}}$  and  $\delta_{\text{dimer}}$  of the H-5 proton as 7.49 and 7.17 ppm, respectively.

$$\delta_{\text{obs}} = \delta_{\text{mon}} \frac{\sqrt{8K_{\text{D}}C_{\text{tot}} + 1} - 1}{4K_{\text{D}}C_{\text{tot}}} + \delta_{\text{dimer}} \frac{(4K_{\text{D}}C_{\text{tot}} + 1) - \sqrt{8K_{\text{D}}C_{\text{tot}} + 1}}{4K_{\text{D}}C_{\text{tot}}} \quad (1)$$

The  $K_{\text{D}}^1$  value is much larger than the binding constant of 2-naphthalenesulfonate with  $\gamma$ -CD,  $38 \text{ M}^{-1}$ , obtained by isothermal calorimetry.<sup>14</sup> On the basis of this and the NMR data,<sup>11</sup> we conclude that the structure of the dimer of **1** is head-to-head, which is stabilized by the mutual inclusion of the pendant groups into the  $\gamma$ -CD cavities of counter molecules. However, the dimerization constant of **1** is much less than the corresponding value of **3**,<sup>11</sup>  $9700(\pm 2500) \text{ M}^{-1}$ , presumably due to loose fitting of the naphthyl group inside the  $\gamma$ -CD cavity.

The  $^1\text{H}$  NMR spectrum of **2** depends highly on the concentration (Figure 1B). As the concentration is higher, the signals from aromatic protons shift significantly. The concentration-dependent chemical shifts of the H-2 proton (Figure 2) fitted well to eq 1, giving the dimerization constant ( $K_{\text{D}}^2$ ) as  $230 \pm 60 \text{ M}^{-1}$  and a  $\Delta\delta_{\infty}$  ( $\delta_{\text{dimer}} - \delta_{\text{mon}}$ ) value of 0.72 ppm.

The c.d. spectrum of **2** exhibits a series of bands, of which most prominent bands are the positive one around 360 nm and the negative one around 280 nm. The magnitude of  $[\theta]$  of the bands becomes greater as the concentration is increased (Figure 3). The dependence of  $[\theta]$  on the concentration of **2** was fitted to eq 1 where all the  $\delta$  values were replaced by  $[\theta]$ . This gave the  $K_{\text{D}}^2$  value as  $300 \pm 30 \text{ M}^{-1}$ , and  $[\theta]$  values at 359 nm were determined as 900 and 14000  $\text{deg cm}^2 \text{ dmol}^{-1}$  for the monomer and dimer of **2**, respectively. The  $K_{\text{D}}^2$  values obtained independently from the NMR and c.d. studies are quite close and the averaged value is  $270 \pm 70 \text{ M}^{-1}$ .

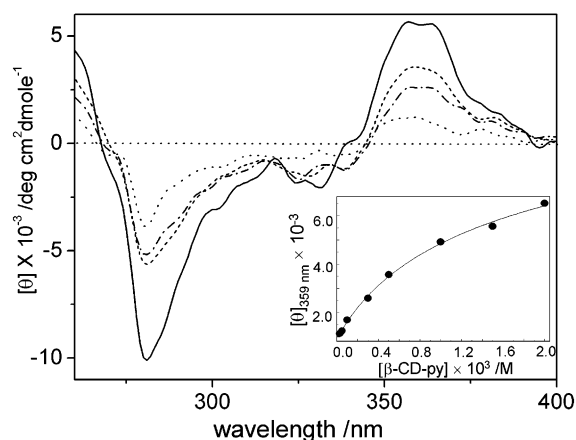


**FIGURE 3.** Concentration dependence of circular dichroism spectra of  $\beta$ -CD-py **2**. The concentrations of **2** are 0.030, 0.30, 0.50, and 2.0 mM (from bottom to top at 360 nm). The inset shows the dependence of the ellipticity at 359 nm on the concentration of **2**.

The size of the pyrene ring is too large to penetrate deeply into the  $\beta$ -CD cavity. The model construction of the pyrene/ $\beta$ -CD complex showed that about half of the pyrene ring protrudes, presumably from the wider secondary face.<sup>15</sup> The reported 1:1 association constant of pyrene with  $\beta$ -CD is in the range of 44–190  $\text{M}^{-1}$ .<sup>16</sup> The observation of the  $K_{\text{D}}^2$  value of about 270  $\text{M}^{-1}$  suggests that the dimer may not be a head-to-tail type, where the pyrene moiety is included from the secondary side of the  $\beta$ -CD cavity of the counter molecule, but would be a head-to-head type. In the head-to-head dimer, the pyrene moieties might be shallowly inserted into the primary face of  $\beta$ -CD cavities of the counter molecules, arranging two pyrenyl groups almost parallel. This arrangement of pyrenyl groups would bring the energetically favorable  $\pi$ - $\pi$  stacking interaction between the groups and stabilize the dimer. The large upfield shift of  $^1\text{H}$  NMR signals of most of the pyrenyl protons (Figure 1B), due to the ring-current effect of the adjacent pyrenyl group in the dimer, is consistent with the dimer structure. Also, the fluorescence spectrum of the 0.50 mM solution of **2** showed an emission band around 510 nm, whereas the band was not observed from the 0.050 mM solution (spectra not shown).<sup>17</sup> We attribute the 510-nm emission band to the excimer band of the pyrenyl group.

**Associations of 1 with  $\beta$ -CD and 2 with  $\gamma$ -CD.** Before studying the heteroassociation between **1** and **2**, we investigated the associations of **1** with  $\beta$ -CD and **2** with  $\gamma$ -CD. The fluorescence intensity of **1** increases upon addition of  $\beta$ -CD in a fashion similar to the fluorescence titration of 6-methoxy-2-naphthalenesulfonate (MNSS) with  $\beta$ -CD.<sup>11</sup> As we used a low concentration ( $1.0 \times 10^{-5} \text{ M}$ ) of **1**, of which the dimerization constant is about 140  $\text{M}^{-1}$ , we can ignore the monomer–dimer equilibrium of

(15) (a) Weying, X.; Demas, N. J.; Degraff, B. A.; Whaley, M. J. *J. Phys. Chem.* **1993**, *97*, 6546. (b) Udachin, K. A.; Ripmeester, J. A. *J. Am. Chem. Soc.* **1998**, *120*, 1080.

(16) (a) Nakjima A. *Spectrochim. Acta, Part A* **1983**, *39*, 913. (b) Hashimoto, S.; Thomas, J. K. *J. Am. Chem. Soc.* **1985**, *107*, 4655.

(17) To avoid the inner filter effect, we excited a 0.50 mM solution of **2** at 388 nm. The fractions of **2** in dimeric form are calculated to be 0.18 and 0.027 for 0.50 and 0.05 mM solutions, respectively, from the dimerization constant of 270  $\text{M}^{-1}$ .

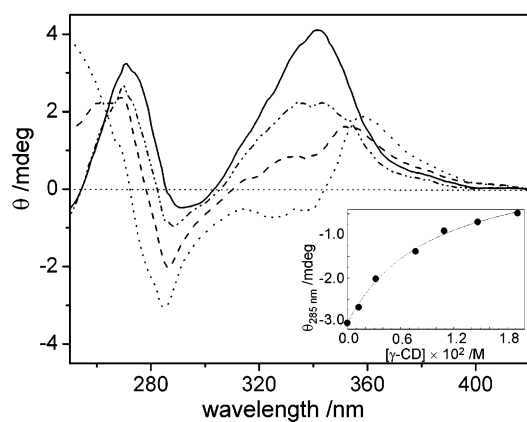


**FIGURE 4.** Effect of  $\gamma$ -CD on the circular dichroism spectra of 0.10 mM  $\beta$ -CD-py **2**. The concentrations of  $\gamma$ -CD are 0.0, 3.2, 10.9, and 19.2 mM (from bottom to top at 340 nm). The inset shows the dependence of the ellipticity at 285 nm on the concentration of  $\gamma$ -CD.

**1** in the analysis of the titration data. For 1:1 association, the change in fluorescence intensity ( $\Delta I$ ) is related to the association constant ( $K_C$ ) and concentration of  $\beta$ -CD by eq 2<sup>11</sup>

$$\Delta I/[\beta\text{-CD}] = K_C \Delta I_\infty - K_C \Delta I \quad (2)$$

where  $\Delta I_\infty$  is the maximum change in fluorescence intensity expected when all of **1** form a complex with  $\beta$ -CD. The fluorescence titration data of **1** with  $\beta$ -CD fitted well to eq 2 (data not shown) and gave a  $K_C^{1/\beta\text{-CD}}$  value of  $270 \pm 20 \text{ M}^{-1}$  and the ratio of fluorescence intensities ( $I_{CD}/I_W = \Delta I_\infty/I_{[\beta\text{-CD}]_0} + 1$ ) of the complex to uncomplexed **1** as 2.4. The  $K_C^{1/\beta\text{-CD}}$  value is slightly smaller than the association constant of the monomeric form of **3** with  $\beta$ -CD,  $430 \pm 50 \text{ M}^{-1}$ , and the  $I_{CD}/I_W$  ratio is slightly larger than that of MNSS, 2.1.<sup>11</sup>

The association of **2** with  $\gamma$ -CD was studied by c.d. titration of a 0.10 mM solution of **2** with  $\gamma$ -CD (Figure 4). The large change of c.d. signals with the concomitant reversal of sign around 330 nm reflects the inclusion of the pyrene moiety of **2** into the cavity of  $\gamma$ -CD.<sup>18</sup> The c.d. titration data fitted to eq 2 after substituting  $\Delta I$  values with  $\Delta[\theta]$  in the equation: we ignored the dimerization equilibrium of **2** as the fraction of monomeric **2** is calculated to be 0.94 from the  $K_D^2$  value of  $270 \text{ M}^{-1}$ . The  $K_C^{2/\gamma\text{-CD}}$  value was obtained as  $100 \pm 30 \text{ M}^{-1}$ .

**Heteroassociation between 1 and 2.** The c.d. spectrum of a mixture of **1** and **2** is remarkably different from the sum of spectra of its components (Figure 5), while the c.d. spectrum of a mixture of **3** and **2** is not much different from the sum of the spectra of its components. These indicate strong heteroassociation between **1** and **2**, whereas **3** and **2** do not exhibit such behavior. To evaluate the association constant ( $K_C^{1/2}$ ) between **1** and **2**, we performed a c.d. titration of a 0.050 mM solution of **2** with **1** varying its concentration up to 2.0 mM (Figure 6). The variation of the ellipticity ( $\theta$ ) at 348 nm on the

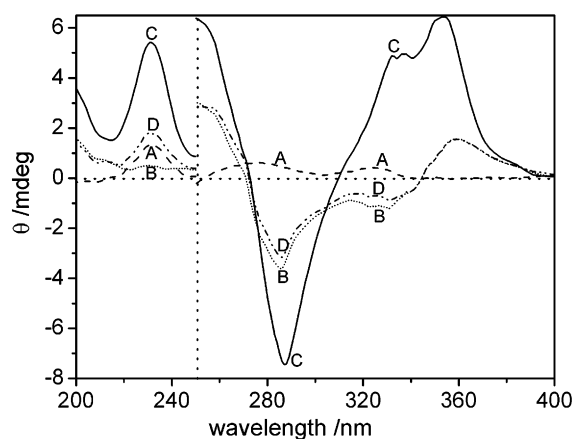


**FIGURE 5.** Circular dichroism spectra of 0.10 mM  $\gamma$ -CD-NS **1** (A), 0.10 mM  $\beta$ -CD-py **2** (B), and a mixture of 0.10 mM **1** and 0.10 mM **2** (C). Spectrum D is the sum of spectra A and B. Cell path lengths are 0.10 cm below 250 nm and 1.0 cm above 250 nm.

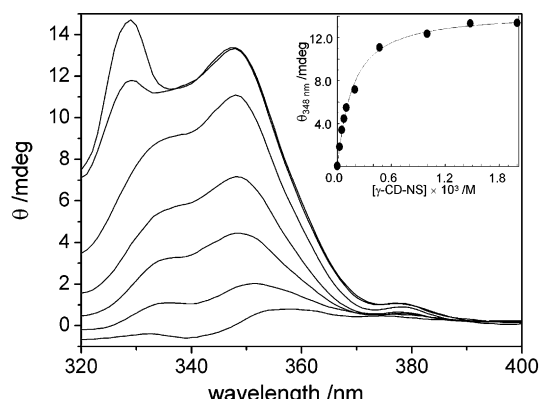


**FIGURE 6.** Circular dichroic titration of 0.050 mM  $\beta$ -CD-py **2** with  $\gamma$ -CD-NS **1**. The concentrations of **1** are 0.0, 0.025, 0.073, 0.19, 0.47, 1.48, and 2.0 mM (from bottom to top). The inset shows the dependence of the molar ellipticity at 348 nm on the concentration of **1**. The peaks around 330 nm at high concentration of **1** are from excess **1**.

concentration of **1** is shown in the inset of Figure 6. Since the naphthyl group does not show significant c.d. signal above 340 nm, the ellipticity change above 340 nm can be attributed to that of **2** affected by the association with **1**. As the fraction of **2** present as the monomeric form in the 0.050 mM solution is calculated to be 0.97, we considered only the equilibria between monomeric **1** and **2**, and the dimerization of **1**. Even under this approximation, the equation relating  $\theta$  and the concentration of **1** becomes a cubic equation due to the similarity in the concentration ranges of **1** and **2**. The regression fitting to the cubic equation was complicated and erratic. Thus, we used a stepwise procedure to evaluate the  $K_C^{1/2}$  value. Using the  $\theta$  value taken at high concentration of **1** as that of the **1/2** complex, we calculated the fraction ( $f_c$ ) of **2** present as the **1/2** complex from the fractional change of  $\theta$  and the total concentration of uncomplexed **1** ( $[\mathbf{1}]_{\text{uncomplexed}}$ ):  $[\mathbf{1}]_{\text{uncomplexed}} = [\mathbf{1}]_o - [\mathbf{2}]_o f_c$ , where subscript "o" denotes total concentrations in mixtures. The concentration of monomeric **1** ( $[\mathbf{1}]_m$ ) was then calculated from  $[\mathbf{1}]_{\text{uncomplexed}}$  and the  $K_D^1$  value. Finally, the  $K_C^{1/2}$  value was

(18) For the same orientation of transition dipole moment of a chromophore bound to CD or in CD complex, the sign of the circular dichroism spectrum is reversed when the chromophore moves from inside to outside of the CD cavity. For details, see ref 11 and references therein.

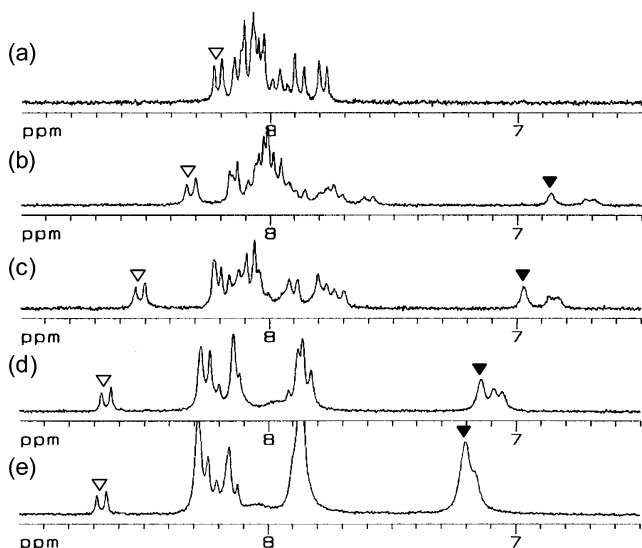


**FIGURE 7.**  $^1\text{H}$  NMR ( $\text{D}_2\text{O}$ ) spectra of the aromatic region of 2.0 mM  $\beta$ -CD-py **2** in the presence of various concentrations of  $\gamma$ -CD-NS **1**. The concentrations of **1** are (a) 0.0, (b) 0.57, (c) 1.36, (d) 3.48, and (e) 8.1 mM. The symbols ▼ and ▽ indicate the signals from the H-5 proton of naphthyl and the H-2 proton of pyrenyl groups, respectively. The positions of H-5 and H-2 protons are shown in Figure 1.

calculated from the relationship of  $K_C^{1/2} = f_c / \{ (1 - f_c) \cdot [\mathbf{1}]_m \}$ . The values obtained at various concentrations of **1** were averaged to obtain  $K_C^{1/2}$  as  $9300 \pm 1600 \text{ M}^{-1}$ . The small uncertainty in the determined  $K_C^{1/2}$  value seems to justify the validity of the procedure and dimerization constants between **1** and **2**. The  $K_C^{1/2}$  value is much larger than the  $K_C^{1/\beta\text{-CD}}$  and  $K_C^{2/\gamma\text{-CD}}$  values, indicating that the **1/2** heterocomplex is stabilized by mutual interaction of the pendant groups with the CD cavities of the counter molecules.

Figure 7 shows  $^1\text{H}$  NMR spectra of the 2.0 mM solution of **2** in the presence of various concentrations of **1**. We had observed that the signals from pyrenyl protons of **2** appear at substantially higher field with the increase of its concentration (Figure 1B). Upon the addition of **1**, the peaks of pyrenyl protons, especially that from H-2, shift downfield. This can be attributed to the dissociation of the dimer of **2** by the **1/2** association. In contrast to the downfield shift of pyrenyl protons in the **1/2** mixtures, the H-5 and H-7 protons of the naphthyl group of **1** appear at much higher field, compared to those of free **1**, when the ratio of  $[\mathbf{2}]/[\mathbf{1}]$  is large (see spectra b and c in Figure 7). This is reminiscent of upfield shifts of the signals of the protons in **1** and **3** upon increasing their concentration, and suggests proximity of the protons to the pyrene ring in the complex.

To obtain better insight of the complex between **1** and **2**, we obtained the energy-minimized structures of the complex by MM2 modeling (Figure 8). It appeared from the modeling in a vacuum that the complex is more stable than the separated molecules by about 190 kJ/mol. It was shown that the naphthyl group of **1** is deeply inserted into the  $\beta$ -CD cavity of **2** and the sulfonate group protrudes from the secondary face of the cavity, but the pyrenyl ring of **2** is partially included into the  $\gamma$ -CD cavity of **1**. It was also suggested that the long axes of the naphthyl and pyrenyl groups are almost parallel with the

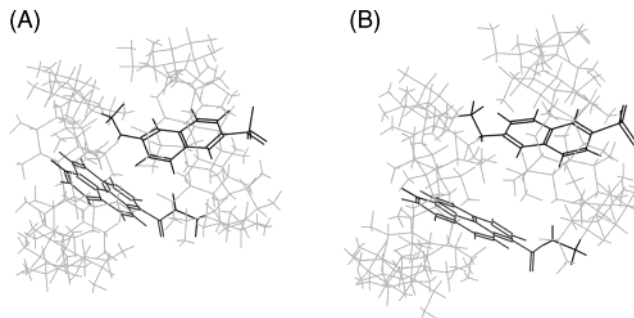


**FIGURE 8.** The energy-minimized structures of the  $\gamma$ -CD-NS **1/** $\beta$ -CD-py **2** complex. Parts A and B differ in the orientation of the naphthyl group inside the  $\beta$ -CD cavity. The energy of part B was lower than that of part A by 8 kJ/mol.

axes of CD cavities where they are included and two CD moieties and thus the aromatic groups are in an oblique arrangement in the complex.

Finally, we would like to suggest a few possible applications of the heteroassociation. One is a chemosensor of high sensitivity. A guest molecule to the CD cavity competes with the pendant groups for the cavity and the heteroassociation equilibrium is shifted by the presence of guests, resulting in the changes of physicochemical properties. Particularly, if complementary pendant groups are excitation energy or the electron donor/acceptor pair, the guest binding would dissociate the heterocomplex and bring about a large fluorescence change by disruption of the excitation transfer. The sensitivity would be much greater than that of self-inclusion or homoassociation systems, in which the change arises mainly from the microenvironmental effect of the fluorescent group. Another use is assembly of CD derivatives modified at both faces: one with a functional group and the other with a complementary linking group. The association involving linking groups gives the assembly having functional groups at both ends. Communication between the functional groups, either with involving or without involving the linking groups, can be investigated by a variety of means.

In summary, 6-*O*-(2-sulfonato-6-naphthyl)- $\gamma$ -CD (**1**) and 6-deoxy-(pyrene-1-carboxamido)- $\beta$ -CD (**2**) were prepared. Homoassociation of **1** and **2**, associations of **1** with  $\beta$ -CD and **2** with  $\gamma$ -CD, and heteroassociation between **1** and **2** were investigated by the combination of  $^1\text{H}$  NMR, circular dichroism (c.d.), and fluorescence spectroscopic methods. The equilibrium constants obtained from this work are summarized in Table 1. Both **1** and **2** form head-to-head type homodimers, but the dimerization constants are much smaller than the corresponding value of 6-*O*-(2-sulfonato-6-naphthyl)- $\beta$ -CD (**3**),  $9700(\pm 2500) \text{ M}^{-1}$ , due to poor size-matching between the pendant groups and the parent CD cavities. The CD derivatives **1** and **2** form a heterocomplex with an association constant of  $9300 \pm 1600 \text{ M}^{-1}$ . The complex is stabilized by the mutual inclusion of the pendant groups into the CD cavities of counter molecules. The facile heteroassociation of CD derivatives demonstrated here would provide a useful strategy for obtaining novel CD-based supramolecular structures for various applications.

TABLE 1. Association Constants in Scheme 2 in 25 °C Aqueous Solutions

entry	systems	notation	$K$ (M <sup>-1</sup> )	method
1	$\gamma$ -CD-NS + $\gamma$ -CD-NS	$K_D^1$	140 ± 50	NMR.
2	$\gamma$ -CD-NS + $\beta$ -CD	$K_C^{1\beta-CD}$	270 ± 20	fluorescence
3	$\beta$ -CD-py + $\beta$ -CD-py	$K_D^2$	270 ± 70	circular dichroism and NMR
4	$\beta$ -CD-py + $\gamma$ -CD	$K_C^{2\gamma-CD}$	100 ± 30	circular dichroism
5	$\gamma$ -CD-NS + $\beta$ -CD-py	$K_C^{1\beta}$	9300 ± 1600	circular dichroism
6 <sup>a</sup>	$\beta$ -CD-NS + $\beta$ -CD-NS	$K_D^3$	9700 ± 2500	circular dichroism and fluorescence

<sup>a</sup> From ref 11.

## Experimental Section

**Materials.**  $\beta$ -CD and  $\gamma$ -CD were recrystallized from water and vacuum dried. Preparations of mono-6-*O*-(2-sulfonato-6-naphthyl)- $\beta$ -CD (**3**) and 6-mono-tosylated  $\beta$ -CD ( $\beta$ -CD-OTs) and purification of sodium 6-hydroxy-2-naphthalenesulfonate were described in a previous paper.<sup>11</sup>

**Mono-6-*O*-(2-sulfonato-6-naphthyl)- $\gamma$ -cyclodextrin (**1**).** Mono-6-*O*-(2-naphthalenesulfonyl)- $\gamma$ -CD (**4**) was prepared by reacting  $\gamma$ -CD and 2-naphthalenesulfonyl chloride in pyridine adapting a literature procedure<sup>19</sup> and purified by reverse-phase chromatography on Lichroprep Rp-18, using a stepwise elution with 0.2 L of aqueous methanols of 10, 20, 30, 40, and 50 vol %. Compound **4** (480 mg, 0.32 mmol) and the disodium salt of 2-sulfonato-naphthalene-6-ol (80 mg, 0.32 mmol), which was obtained by precipitation with acetone from an equimolar mixture of 6-hydroxy-2-naphthalene sulfonate and NaOH, were reacted in 2 mL of DMSO at 80 °C for 6 h under N<sub>2</sub> atmosphere. After precipitation with acetone, the precipitate was dissolved in water and purified by anion exchange chromatography on Sephadex DEAE A-25, using a linear gradient of NaCl (0–0.4 M). UV and optically active fractions were collected and concentrated to dryness. The salt was removed by filtration after selective solubilization of the product in DMF. After DMF was evaporated off, the product was dissolved in water, ultrafiltrated through a MWCO 1000 cellulose membrane, and finally freeze-dried to obtain 117 mg (yield 24%) of the desired product. **1**: mp 247 °C dec; UV(H<sub>2</sub>O)  $\lambda_{max}/nm$  (log  $\epsilon/M^{-1} cm^{-1}$ ) 278 (3.76), 313 (3.03), 328 (2.94); <sup>1</sup>H NMR (3.0 mM in D<sub>2</sub>O)  $\delta$  8.35 (s, 1H), 7.95 (m, 3H), 7.39 (m, 2H), and  $\gamma$ -CD resonances.; Anal. Calcd for C<sub>58</sub>H<sub>85</sub>NaO<sub>43</sub>S·8H<sub>2</sub>O (with 2.0% NaCl): C, 40.90; H, 5.98. Found: C, 40.79; H, 6.01. ESI-MS *m/z* found 785.1921, calcd for [M + 2Na<sup>+</sup>]<sup>2+</sup> 785.1939.

**6-Deoxy-(pyrene-1-carboxamido)- $\beta$ -Cyclodextrin (**2**).** Mono-6-deoxy-6-amino- $\beta$ -CD ( $\beta$ -CD-6-NH<sub>2</sub>) was prepared from  $\beta$ -CD-OTs via  $\beta$ -CD-6-azide intermediate.<sup>20</sup> Compound **2** was prepared by a procedure for the amide coupling of an amine with an acid as follows.<sup>21</sup>  $\beta$ -CD-6-NH<sub>2</sub> (350 mg, 0.31 mmol) and an equimolar amount of 1-pyrenecarboxylic acid were dissolved in dry DMF (15 mL) and the solution was cooled to 0 °C. To this were added solutions of dicyclohexylcarbodiimide (64 mg, 0.31 mmol) in 1.0 mL of DMF and 1-hydroxybenzot-

riazole (42 mg, 0.31 mmol) in 1.0 mL of DMF. The resulting solution was stirred at 0 °C for 2 h and then at room temperature for 48 h. After dicyclohexylurea was filtered off, the reaction mixture was concentrated to half volume by evaporation and precipitated by adding acetone to obtain 450 mg of crude product. The desired product was separated by reverse-phase column chromatography, using Lichroprep Rp-18 (40–63  $\mu$ m). Stepwise elution with 0.0, 30, 50, 70, and 100 vol % of aqueous MeOH was employed. At 70 vol % of aqueous MeOH, the UV and optically active fractions of  $R_f$  0.58 (*n*-PrOH:H<sub>2</sub>O:6 M NH<sub>4</sub>OH 6:2:3 (v/v), TLC; silica gel 60F<sub>254</sub>) were eluted out. Column chromatography was repeated once more to obtain 170 mg (40% yield) of analytically pure title compound. **2**: mp  $\geq$ 270 °C dec; UV(H<sub>2</sub>O)  $\lambda_{max}/nm$  (log  $\epsilon/M^{-1} cm^{-1}$ ) 242 (4.74), 266 (4.32), 276 (4.55), 326 (4.28), 342 (4.44), 376 (3.26); <sup>1</sup>H NMR (3.0 mM in D<sub>2</sub>O)  $\delta$  8.24 (d, 1H, py), 7.96–8.04 (m, 6H, py), 7.91 (d, 1H, py), 7.66 (d, 1H, py), 5.03–5.30 (m, 7H, H1 of  $\beta$ -CD), 2.57–4.55 (m, 42H, H2, 3, 4, 5, 6a, 6b protons of  $\beta$ -CD), Anal. Calcd for C<sub>59</sub>H<sub>79</sub>NO<sub>35</sub>: C, 52.02; H, 5.85; N, 1.03. Found: C, 52.13; H, 5.89; N, 1.02.

**Spectroscopic Measurements.** <sup>1</sup>H NMR spectra were obtained with a 250-MHz NMR spectrometer, using 3-(trimethylsilyl)propionic acid-*d*<sub>4</sub> sodium salt (TSP,  $\delta = 0$ ) as an external standard. For taking circular dichroism (c.d.) spectra, the cell path length was varied from 0.010 to 10.0 cm depending on the concentration and wavelength region to maintain absorbance below 3. An aqueous solution of 0.1 M NaCl was used as a blank for c.d. spectral measurements. The bandwidth was set at 2 nm and the response time was 2 s. Spectra were scanned 10 times at the speed of 50 nm/min, averaged, and then smoothed. All spectroscopic measurements were carried out at 25 °C, using the appropriate temperature controller. Unless otherwise specified, the ionic strength of the solutions was fixed at 0.1 M with NaCl. The molecular modeling calculations were carried out with the MM2 force field.

**Acknowledgment.** This work was supported by CRM/KOSEF, Korea University. The authors thank Min-Hee Lee for her technical assistance in the synthesis of **1** and the Korea Basic Science Institute for ESI-MS measurements.

**Supporting Information Available:** Tables of atomic coordinates of the calculated structures given in Figure 8. This material is available free of charge via the Internet at <http://pubs.acs.org>.

JO034623H

(19) Ueno, A.; Tomita, Y.; Osa, T. *Chem. Lett.* **1983**, 1636.

(20) Ashton, P. R.; Koniger, R. *J. Org. Chem.* **1996**, 61, 903.

(21) (a) Tesler, J.; Cruickshank, K. A.; Schanze, K. S.; Netzel, T. C. *J. Am. Chem. Soc.* **1989**, 111, 7221. (b) Ueno, A.; Takahashi, M.; Nagano, Y.; Shibano, H.; Aoyagi, T.; Ikeda, H. *Macromol. Rapid Commun.* **1998**, 19, 315.